Cell

Cdk-Inhibitory Activity and Stability of $p27^{Kip1}$ Are Directly Regulated by Oncogenic Tyrosine Kinases

Matthias Grimmler,[2,6,7] Yuefeng Wang,[3,7] Thomas Mund,[2,7] Zoran Cilenšek,[2,7] Eva-Maria Keidel,[2] M. Brett Waddell,[4] Heidelinde Jäkel,[1] Michael Kullmann,[1] Richard W. Kriwacki,[3,5,*] and Ludger Hengst[1,2,*]
[1] Division of Medical Biochemistry, Biocenter, Innsbruck Medical University, Fritz Pregl Strasse 3, A-6020 Innsbruck, Austria
[2] Max Planck Institute of Biochemistry, Am Klopferspitz 18, D-82152 Martinsried, Germany
[3] Department of Structural Biology
[4] Hartwell Center for Bioinformatics and Biotechnology
St. Jude Children's Research Hospital, 332 North Lauderdale Street, Memphis, TN 38105, USA
[5] Department of Molecular Sciences, University of Tennessee Health Sciences Center, Memphis, TN 38105, USA
[6] Present address: Institute of Biochemistry, Biocenter, University of Würzburg, Am Hubland, D-97074 Würzburg, Germany.
[7] These authors contributed equally to this work.
*Correspondence: richard.kriwacki@stjude.org (R.W.K.), ludger.hengst@i-med.ac.at (L.H.)
DOI 10.1016/j.cell.2006.11.047

SUMMARY

$p27^{Kip1}$ controls cell proliferation by binding to and regulating the activity of cyclin-dependent kinases (Cdks). Here we show that Cdk inhibition and p27 stability are regulated through direct phosphorylation by tyrosine kinases. A conserved tyrosine residue (Y88) in the Cdk-binding domain of p27 can be phosphorylated by the Src-family kinase Lyn and the oncogene product BCR-ABL. Y88 phosphorylation does not prevent p27 binding to cyclin A/Cdk2. Instead, it causes phosphorylated Y88 and the entire inhibitory 3_{10}-helix of p27 to be ejected from the Cdk2 active site, thus restoring partial Cdk activity. Importantly, this allows Y88-phosphorylated p27 to be efficiently phosphorylated on threonine 187 by Cdk2 which in turn promotes its SCF-Skp2-dependent degradation. This direct link between transforming tyrosine kinases and p27 may provide an explanation for Cdk kinase activities observed in p27 complexes and for premature p27 elimination in cells that have been transformed by activated tyrosine kinases.

INTRODUCTION

The Cdk-inhibitor $p27^{Kip1}$ is an intrinsically unstructured protein (IUP; Lacy et al., 2004) that controls cell proliferation by binding to and regulating the activity of cyclin-dependent kinases (Cdks). Usually, binding of p27 inactivates the kinase; however, p27 was surprisingly also found to be associated with active cyclin D holoenzymes (Sherr and Roberts, 1999). p27 level is frequently controlled by regulated translation and proteolysis (Hengst and Reed, 1996; Pagano et al., 1995). The protein is abundant in quiescent (G_0) cells (Hengst and Reed, 1998; Sherr and Roberts, 1999) and is relatively stable in G_0 and early G_1 phase. p27 becomes unstable as cells progress toward S phase (Hengst and Reed, 1996; Pagano et al., 1995). p27 degradation is initiated by different ubiquitin ligases. Among these, the KPC1 complex ubiquitinates free unphosphorylated p27 (Kamura et al., 2004; Kotoshiba et al., 2005), whereas Skp2-dependent E3 ligase complexes target p27 only after phosphorylation on threonine 187 (T187) (Bloom and Pagano, 2003; Sabile et al., 2006). Active cyclin E/Cdk2 can phosphorylate T187 of cyclin/Cdk-bound p27 (Bloom and Pagano, 2003). While free and active cyclin/Cdk2 efficiently phosphorylates Cdk-bound p27, p27-bound Cdk2 is catalytically inactive due to p27-mediated remodeling of the catalytic cleft and displacement of ATP (Pavletich, 1999). This suggested that degradation by the SCF-Skp2 pathway may require p27-free cyclin E/Cdk2 and led to the puzzle of how p27 degradation can be initiated in G_1.

We now report that p27 can be phosphorylated on a tyrosine residue at position 88 (Y88) within its Cdk-binding domain. This phosphorylation caused the inhibitory 3_{10}-helix of p27 to be ejected from the ATP-binding pocket of Cdk2. Y88-phosphorylated p27 still bound to cyclin/Cdk complexes, but the associated kinase retained significant catalytic activity. Furthermore, Y88-phosphorylated p27 became an efficient substrate for phosphorylation on T187 by Cdk2 within the trimeric complex. Thus, Y88 phosphorylation may trigger p27 ubiquitination in the absence of free cyclin/Cdk2 and may initiate SCF-Skp2-dependent p27 degradation at the G_1/S transition.

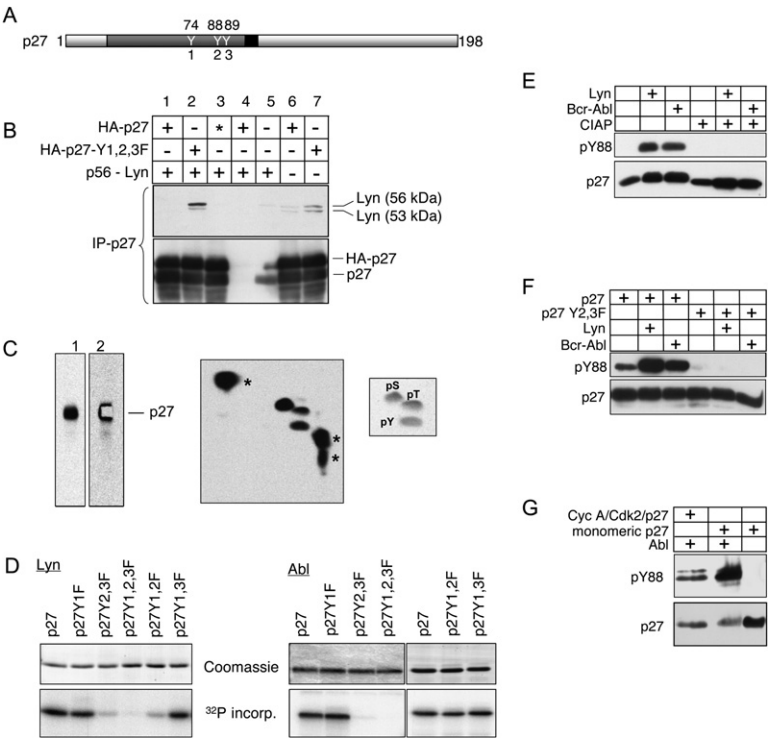

Figure 1. p27^{Kip1} Binds the Tyrosine Kinase Lyn and Is Phosphorylated on Tyrosine

(A) All tyrosine residues (indicated as Y) of p27 are located in the Cdk-inhibitory domain (dark gray). A proline-rich SH3-binding element (residues 91–96) is represented as a black box.

(B) Lyn binds to a p27 mutant protein lacking all three tyrosines. p27, a mutant of p27 where the tyrosines were exchanged to phenylalanine, and an activated allele of the 56 kDa isoform of Lyn (Y508F) were expressed in HeLa cells as indicated. Cells were collected 24 hr post-transfection, and p27 was immunoprecipitated (lanes 1–3 and 5–7, anti-p27 polyclonal antibody; lane 4, immunoprecipitation with control IgG). Immunoprecipitates were separated by SDS-PAGE, and p27-associated Lyn (upper panel) and precipitated p27 (lower panel) were detected in western blots. In lane 3, a SH3 domain-binding-deficient mutant of p27 (P94G, P95G, K96A; *) was coexpressed with activated Lyn.

(C) p27 is phosphorylated on tyrosine. 2D phosphoamino acid analysis of immunoprecipitated p27 is shown. HeLa cells transfected with untagged p27 were labeled with [^{32}P]-ortho-phosphate. Protein extracts were boiled, and p27 was immunoprecipitated and separated by SDS-PAGE. Autoradiography of immunoprecipitated p27 is shown before (left panel, left lane) and after (right lane) excision of the protein. Excised p27 was hydrolyzed and subjected to 2D cellulose thin-layer electrophoresis. The autoradiography (middle) shows phosphate incorporation into serine, threonine, and tyrosine. Partially hydrolyzed phosphopeptides are indicated by asterisks. The migration of standards representing phosphoserine, -threonine, or -tyrosine is also shown after ninhydrin staining (right panel).

(D) Lyn and Abl phosphorylate Y88 of p27 in vitro. Equal amounts of p27 or mutant p27 (tyrosine residues exchanged to phenylalanine; Y1F: Y in position 74 exchanged to F; Y2: Y in position 88; and Y3: Y in position 89) were incubated with recombinant constitutively active Lyn or Abl kinase at 30°C in the presence of γ-[^{32}P]-ATP. Proteins were separated by SDS-PAGE and detected by Coomassie staining (upper panel). The amount of incorporated ^{32}P was shown by autoradiography (lower panel).

(E) p27 is phosphorylated on Y88 in vivo. HA-tagged p27 was coexpressed in 293T cells with Lyn (Y508F) or p210 BCR-ABL kinase. Anti-HA immunoprecipitates were incubated with (+) or without calf intestinal alkaline phosphatase (CIAP) and analyzed by western blotting using purified polyclonal anti-phospho-Y88 p27 antibodies. The same blot was subsequently probed with an HRP-conjugated anti-p27 antibody.

(F) p27 tyrosine phosphorylation is enhanced by overexpression of Lyn or BCR-ABL kinase. MCF7 cells transiently coexpressing either HA-tagged p27 or mutant HA-tagged p27 (Y88F and Y89F, as indicated) and BCR-ABL or Lyn kinase were treated with sodium orthovanadate for 4 hr. Tagged p27 species were immunoprecipitated with anti-HA antibodies and analyzed with purified polyclonal anti-phospho-Y88 p27 antibodies. The same membrane was subsequently probed with an HRP-conjugated anti-p27 antibody.

(G) Monomeric p27 is a better substrate for Abl kinase than p27 bound to a cyclin A/Cdk2 complex. Stable complexes of p27 bound to cyclin A/Cdk2 were isolated by gel filtration chromatography. Equal amounts of monomeric or cyclin A/Cdk2-bound p27 were incubated with or without Abl kinase as indicated, and proteins were separated by SDS-PAGE and analyzed for Y88 phosphorylation by using a monoclonal pY88-specific antibody.

RESULTS

p27 Is Phosphorylated on Tyrosine

While searching for p27-interacting proteins, we affinity purified Grb2 from HeLa cell extracts. The C-terminal SH3 domain of Grb2 bound to a proline-rich segment of p27 as shown previously (M.G., unpublished data; Moeller et al., 2003; Sugiyama et al., 2001). We speculated that additional SH3 domain proteins might bind p27 and found that the SH3 domain of the tyrosine kinase Lyn bound to p27.

Within the Cdk-inhibitory domain the p27 sequence contains three tyrosine residues near the proline-rich SH3-binding element (Figure 1A). To investigate if phosphorylation of tyrosines influenced binding of p27 to the kinase, we exchanged these tyrosine residues to phenylalanine. The binding of p27 to an activated 56 kDa isoform of Lyn was strongly enhanced when mutant p27 was expressed (Figure 1B). Without Lyn overexpression, p27 could still coprecipitate endogenous Lyn (Figure 1B), which may be catalytically inactive and therefore more stably bound to p27. These observations suggested that p27 is a substrate of tyrosine kinases.

To investigate tyrosine phosphorylation of p27, we first performed a phosphoamino acid analysis of immunoprecipitated, overexpressed p27 from [^{32}P]-*ortho*-phosphate-labeled HeLa cells. While phosphoserine was most abundant, phosphothreonine and phosphotyrosine were detected at similar and significant levels (Figures 1C and S1; Table S2). Recently, tyrosine phosphorylation of p27 was also reported in NB4 promyelocytic leukemia cells

(Kardinal et al., 2006). We next determined that the nonreceptor tyrosine kinases Lyn and Abl could phosphorylate p27 in vitro (Figure 1D).

To identify the tyrosine residues phosphorylated by Lyn or Abl, we replaced combinations of one, two, or all three tyrosine residues of p27 with phenylalanine. Only mutant proteins that retained Y88 were efficiently phosphorylated in vitro (Figure 1D). p27 lacking tyrosine 74 and tyrosine 89 was phosphorylated to approximately the same extent as wild-type (WT) p27. Thus, Y88 is a major phosphoacceptor site of p27. Lyn did not efficiently phosphorylate proteins in which Y88 was replaced with phenylalanine, whereas Abl still phosphorylated proteins that lacked Y88 but retained Y89, although it did so with reduced efficiency (Figure 1D). The similarity of the level of phosphorylation of WT p27 and of the mutant protein that contained only Y88 indicated that on average only one tyrosine per inhibitor molecule becomes phosphorylated. Y88 is therefore a principal phosphoacceptor site of p27 in vitro.

We next investigated whether p27 is also a substrate for Lyn and Abl kinases in vivo by generating phosphospecific antisera against phosphotyrosine-containing peptides (Figures 1E and S2). In the absence of overexpressed tyrosine kinases, Y88 phosphorylation was readily detected in immunoprecipitated p27 of MCF7 cells (Figure 1F), whereas longer exposures were required to detect Y88 phosphorylation in 293T cells (Figure 1E; data not shown). When p27 was coexpressed with constitutively active Lyn (mutant Y508F) or p210 BCR-ABL, the level of phosphorylation was significantly increased (Figures 1E and 1F). Thus, phosphorylation of Y88 on p27 occurs in vivo and is enhanced by overexpression of these tyrosine kinases.

Y88 is located in the inhibitory 3_{10}-helix of p27 and becomes deeply buried within the ATP-binding pocket within the catalytic cleft of Cdk2 (Pavletich, 1999; Russo et al., 1996). To determine whether p27 within cyclin/Cdk complexes could still be phosphorylated on Y88, we purified p27/cyclin A/Cdk2 ternary complexes using two successive rounds of size-exclusion chromatography (SEC). Equal amounts of monomeric or cyclin A/Cdk2-bound p27 were incubated with Abl kinase. While monomeric p27 was a better substrate for Abl phosphorylation, tyrosine phosphorylation of cyclin A/Cdk2-bound p27 was clearly detected (Figure 1G). The intrinsic flexibility of p27 (Lacy et al., 2004) may enable Y88 to fluctuate to an 'open' conformation that allows phosphorylation by tyrosine kinases.

Y88-Phosphorylated p27 Binds Cyclin/Cdk Complexes

Phosphorylation of Y88 might prevent binding of p27 to cyclin/Cdk complexes or induce a different mode of binding. We used SEC (Figure 2A) and surface plasmon resonance (SPR; Table 1) to characterize interactions between tyrosine-phosphorylated p27 and Cdk complexes. The results of SEC showed that both unmodified p27 and Y88-phosphorylated p27 (pY88-p27) bound to recombinant cyclin A/Cdk2 (Figure 2A). To exclude phosphorylation of Y89 in SPR analysis, we used a protein where tyrosine 89 was replaced by phenylalanine ($p27^{Y89F}$). Cdk inhibition by $p27^{Y89F}$ was indistinguishable from that of WT p27 (data not shown). Cyclin A/Cdk2 bound to immobilized $p27^{Y89F}$ and pY88-$p27^{Y89F}$ with similar values of the equilibrium dissociation constant (K_D of 4.4×10^{-9} M versus 3.8×10^{-9} M, respectively; Table 1; Figure S3). Y88 phosphorylation did not influence the binding of isolated cyclin A to $p27^{Y89F}$ (K_D of 49.6×10^{-9} M versus 40.3×10^{-9} M for $p27^{Y89F}$ and pY88-$p27^{Y89F}$, respectively; Table 1; Figure S5). This interaction may be especially important for the trimeric complex formation, as p27 bound to cyclin A in the absence of Cdk2 but did not form a stable complex with Cdk subunits (Hall et al., 1995). In contrast, isolated Cdk2 bound to pY88-$p27^{Y89F}$ significantly more weakly ($K_D = 4.52 \times 10^{-6}$ M) than it did to $p27^{Y89F}$ ($K_D = 248 \times 10^{-9}$ M) (Table 1 and Figure S4), suggesting that phosphorylation of Y88 weakened the binding of p27 to Cdk2. Finally, we also demonstrated that Y88-phosphorylated p27 still bound to cyclin/Cdk complexes in vivo, as endogenous Y88-phosphorylated p27 in K562 cells coimmunoprecipitated in complexes with cyclin D1 and cyclin E1 (Figure 2B).

pY88-p27-Bound Cyclin/Cdk Complexes Retain Catalytic Activity

Y88 phosphorylation weakens binding to isolated Cdk2, which indicates that Y88 phosphorylation alters the p27/Cdk interaction and inhibition. Indeed, pY88-$p27^{Y89F}$ was a slightly less potent inhibitor of Cdk2 than unphosphorylated $p27^{Y89F}$ (Figures 2C, S7A, and S7B). Importantly, in contrast to the complete inhibition observed with $p27^{Y89F}$, Cdk2 exhibited significant kinase activity (20% of maximal) even when saturated with pY88-$p27^{Y89F}$ (Figure 2C). This observation may be biologically relevant and may provide an explanation for a number of reports that describe active Cdk2 kinase coimmunoprecipitating with p27 (Ciarallo et al., 2002; Radeva et al., 1997).

The retinoblastoma protein (Rb) is recruited as a substrate to cyclin A/Cdk2 through interactions between its K/RXL motif and an exposed hydrophobic pocket on cyclin A (Schulman et al., 1998). As p27 also occupies this pocket on cyclin A, we investigated Rb phosphorylation by pY88-p27. With Rb as a Cdk2 substrate Y88 phosphorylation also diminished inhibitory potency of p27 (Figure 2D). Phosphorylation of Y88 also impaired the ability of p27 to inhibit the Rb-kinase activity of a single-chain cyclin D1/Cdk4-fusion protein (Figure 2E). Therefore, impaired Cdk inhibition is a general consequence of p27 Y88 phosphorylation.

pY88 of p27 Is Ejected From the Cdk2 Catalytic Cleft

We used solution NMR spectroscopy to elucidate the structural consequences of pY88 phosphorylation. We studied the N-terminal Cdk-inhibitory domain p27-KID^{Y89F} because the C terminus (residues 105–198) did not influence Cdk-inhibitory properties of p27 variants (compare Figures 2C and S7B). While several p27-KID subdomains, including the 3_{10}-helix, are folded prior to binding

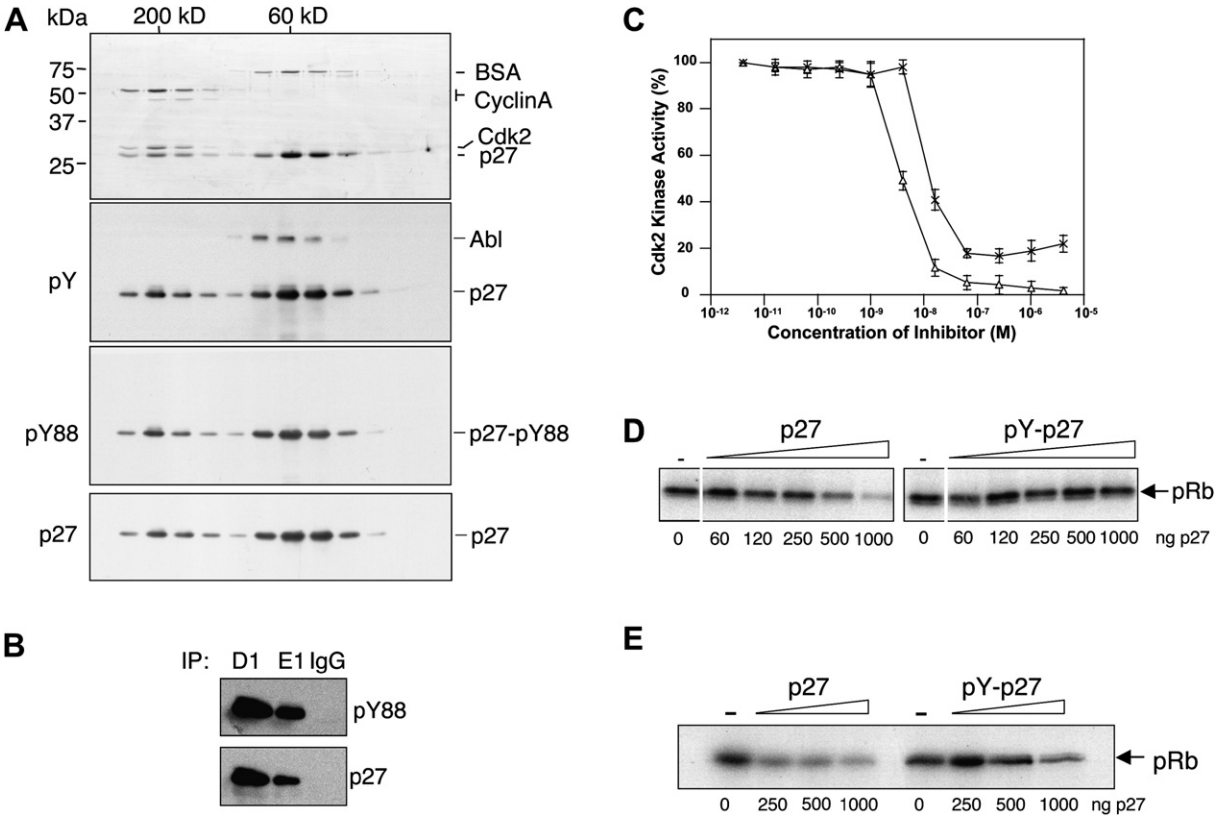

Figure 2. Y88-Phosphorylated p27 Binds Cdk Complexes

Cdks are partially active even when saturated with Y88 phosphorylated p27.

(A) Tyrosine-phosphorylated and unphosphorylated recombinant p27 were mixed in a ratio of 1:1 and subsequently incubated with cyclin A/Cdk2. Protein complexes were separated by gel filtration from unbound p27. Fractions were analyzed by Coomassie staining (upper panel) and western blotting (lower panels) using anti-phosphotyrosine antibodies (pY) reacting with p27 and Abl, a sequence-specific polyclonal pY88-p27 antibody, and a HRP-coupled anti-p27 antibody as indicated.

(B) pY88-p27 binds cyclin D and cyclin E complexes in vivo. Cyclin D1 and cyclin E1 complexes were immmunoprecipitated from the K562 cell lysates. Precipitates were analyzed using anti-pY88-p27 and HRP-conjugated anti-p27 antibodies.

(C) Results of cyclin A/Cdk2 kinase-inhibition assays using $p27^{Y89F}$ (triangles) and pY88-$p27^{Y89F}$ ("X" symbols) with histone H1 as substrate. The error bars correspond to ± one standard deviation of the mean based on triplicate measurements.

(D) Rb-kinase of cyclin A/Cdk2 remains partially active in the presence of tyrosine-phosphorylated p27. Equal amounts of tyrosine-phosphorylated (pY-p27) or mock-treated recombinant p27 (top panel) were incubated with purified cyclin A/Cdk2 and investigated for their ability to inhibit kinase activity using Rb as a substrate. The incorporation of ^{32}P into Rb is shown. The inhibitory activity of phosphorylated p27 is about 10-fold reduced upon tyrosine phosphorylation.

(E) As in (D), but a single-chain cyclin D1/Cdk4 kinase was used with pRb as a substrate.

cyclin/Cdk complexes, overall the polypeptide is intrinsically disordered and dynamic (Lacy et al., 2004; Sivakolundu et al., 2005; Figure S8A). Upon binding to cyclin A/Cdk2, both p27-KID^{Y89F} and pY88-p27-KID^{Y89F} adopted a conformation (Figures S8B and S8D) largely consistent with that of p27-KID bound to cyclin A/Cdk2 in crystals (Russo et al., 1996). Strikingly, however, the NMR data showed that while locally folded (Figure S9), residues within the 3_{10}-helix of pY88-p27-KID^{Y89F} did not interact with Cdk2 (Figures 3B, S8C, and S8D). These results showed that phosphorylation of Y88 caused the p27 3_{10}-helix to be ejected from the ATP-binding pocket of Cdk2 (compare Figures 3A and 3B). Importantly, this local structural disruption did not affect the binding of other p27 residues to cyclin A/Cdk2. Thus, ejection of the 3_{10}-helix from the active site allowed Cdk2 to retain significant activity when cyclin A/Cdk2 was bound to pY88-p27^{Y89F} (and to pY88-p27-KID^{Y89F}). The activity of pY88-bound Cdk2 may be reduced relative to that of the binary cyclin A/Cdk2 complex because the structure of the N-terminal, β sheet lobe of Cdk2 is altered by the binding of p27, domain 2 (Russo et al., 1996).

Y88 Phosphorylation Promotes Cdk2-Mediated Phosphorylation of p27 at T187

p27 is not only an inhibitor but is also a substrate of Cdk2. When Cdk2 phosphorylates T187, this modification promotes p27 degradation by the SCF-Skp2 ubiquitin-proteasome pathway (Bloom and Pagano, 2003). Binding to the Cdk complex appears to be important for

Table 1. Surface Plasmon Resonance (SPR) Analysis of p27 Species Binding to Cyclin A, Cdk2, and Cyclin A/Cdk2

Protein Interaction	k_a (M^{-1} s^{-1}) × 10^3	k_d (s^{-1}) × 10^{-4}	K_D (M)
$p27^{Y89F}$ + cyclin A/Cdk2[a]	–	–	4.4 (± 0.1) × 10^{-9}
pY88-$p27^{Y89F}$ + cyclin A/Cdk2[a]	–	–	3.8 (± 0.1) × 10^{-9}
$p27^{Y88,89F}$ + cyclin A/Cdk2[a]	–	–	5.8 (± 0.1) × 10^{-9}
$p27^{Y89F}$ + Cdk2[b]	1.51 ± 0.01	3.75 ± 0.04	2.48 (± 0.04) × 10^{-7}
pY88-$p27^{Y89F}$ + Cdk2[b]	0.73 ± 0.01	33.03 ± 0.12	4.52 (± 0.08) × 10^{-6}
$p27^{Y89F}$ + cyclin A[a]	–	–	49.6 (± 0.1) × 10^{-9}
pY88-$p27^{Y89F}$ + cyclin A[a]	–	–	40.3 (± 0.1) × 10^{-9}
p27-KID^{Y89F} + cyclin A/Cdk2[a]	–	–	2.9 (± 0.1) × 10^{-9}
pY88-p27-KID^{Y89F} + cyclin A/Cdk2[a]	–	–	2.7 (± 0.1) × 10^{-9}
p27-KID^{Y89F} + Cdk2[b]	2.31 ± 0.01	4.41 ± 0.05	1.91 (± 0.03) × 10^{-7}
pY88-p27-KID^{Y89F} + Cdk2[b]	1.16 ± 0.01	10.42 ± 0.05	8.98 (± 0.12) × 10^{-7}
p27-KID^{Y89F} + cyclin A[a]	–	–	38.7 (± 0.1) × 10^{-9}
pY88-p27-KID^{Y89F} + cyclin A[a]	–	–	30.3 (± 0.1) × 10^{-9}

Equilibrium dissociation constants and kinetic rate constants for unphosphorylated and phosphorylated $p27^{Y89F}$ and p27-KID^{Y89F} binding to cyclin A/Cdk2, Cdk2, and cyclin A, as well as $p27^{Y88,89F}$ binding to cyclin A/Cdk2 are shown as determined using surface plasmon resonance (SPR).

[a] Equilibrium dissociation constants were determined by equilibrium affinity analysis. Biphasic binding was observed by kinetic analysis; therefore, kinetic rate constants were not determined.

[b] Equilibrium dissociation constants were calculated from kinetic rate constants as $K_D = k_d / k_a$, where k_a is the association rate constant, and k_d is the dissociation rate constant.

phosphorylation of p27, as a mutant of p27 that lacked stable cyclin/Cdk interaction and that was unable to inhibit the kinase complex (data not shown) was not efficiently phosphorylated by Cdk2 (Figure 4A, p27-ΔCdk).

As Cdk2 was partially active when pY88-p27 was bound, we determined whether pY88-p27 was a better substrate for Cdk phosphorylation than unphosphorylated p27. p27 was first phosphorylated on Y88 with Abl kinase. Phosphorylated or mock-treated p27 was incubated first with cyclin A/Cdk2 and then with [^{32}P] γ-ATP, and phosphorylation of p27 by Cdk2 was determined. Phosphorylation of unmodified p27 by Cdk2 was marginal, whereas pY88-p27 was efficiently and exhaustively phosphorylated by Cdk2 (Figures 4A and S13). Using phospho-T187-p27-specific antibodies we confirmed that this increased phosphorylation by Cdk2 involved increased phosphorylation of T187 (Figure 4B). Importantly, enhanced T187 phosphorylation was specific for phosphorylation of Y88, as

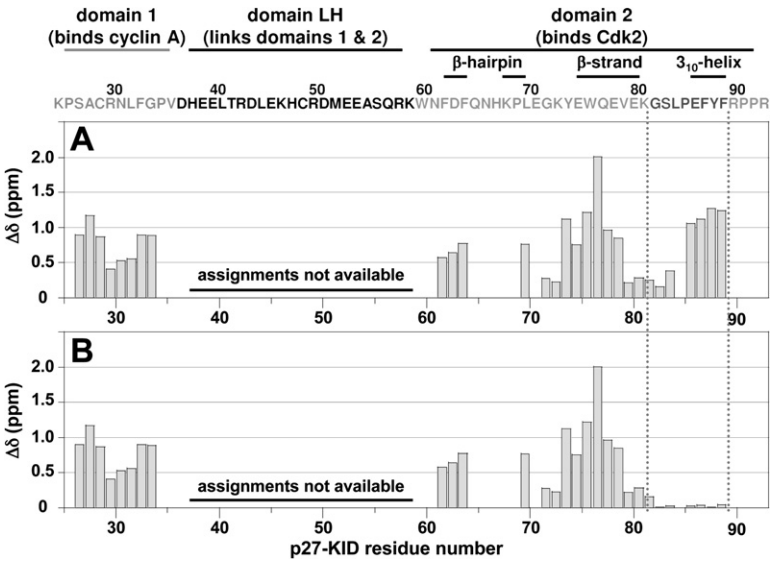

Figure 3. Phosphorylation of p27 Y88 Ejects the 3_{10}-Helix from the ATP-Binding Pocket of Cdk2

NMR chemical shift differences (Δδ) between (A) free p27-KID^{Y89F} and p27-KID^{Y89F} bound to cyclin A/Cdk2 are compared with those for (B) free pY88-p27-KID^{Y89F} and pY88-p27-KID^{Y89F} bound to cyclin A/Cdk2. Δδ values were calculated using the equation: $\Delta\delta = [(\Delta\delta\ H_N)^2 + 0.0289 \times (\Delta\delta\ N_H)^2]^{1/2}$. The location of these domains within the sequence of p27-KID is indicated at the top of the figure. Amino acid residues are indicated using the single letter code.

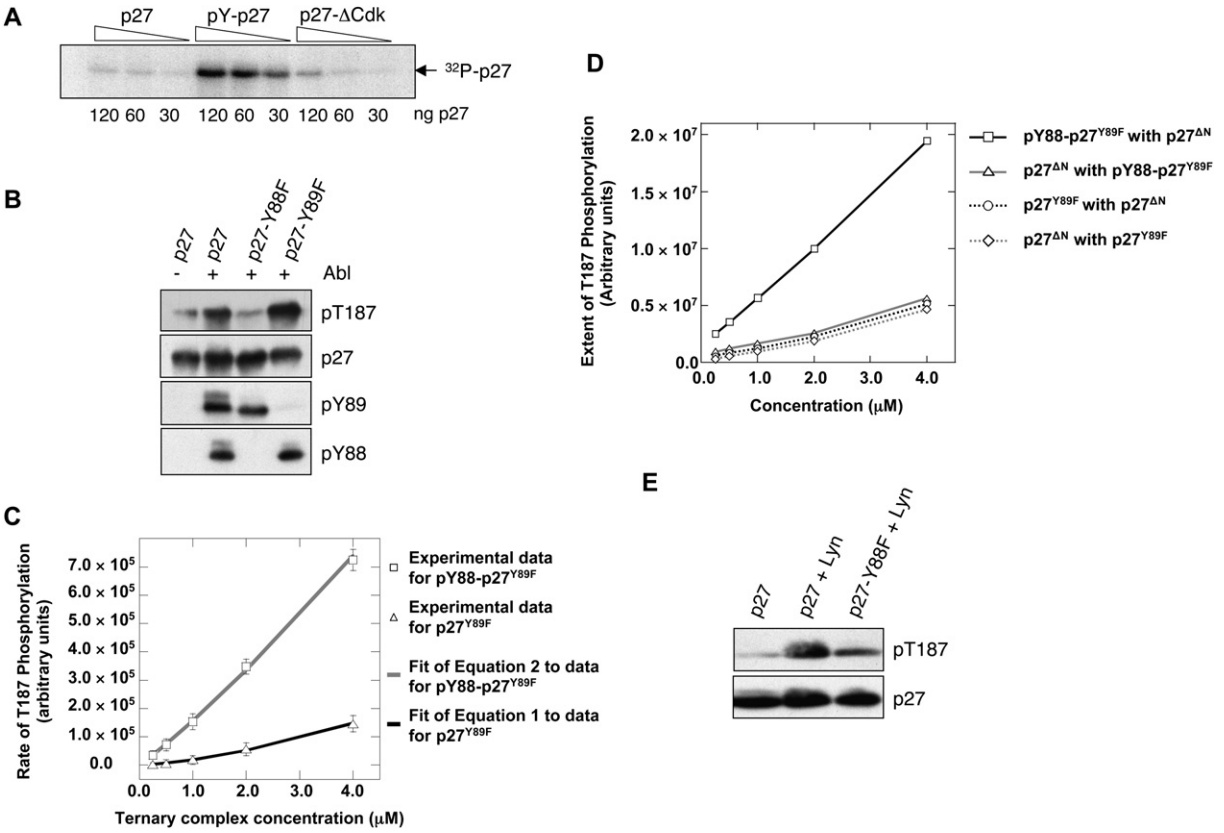

Figure 4. Y88 Phosphorylation Primes p27 for T187 Phosphorylation

(A) Y88-phosphorylated p27 is a superior substrate for Cdk2. pY88-p27^{Y89F} and p27^{Y89F} were compared to a p27 mutant that is unable to bind cyclin A/Cdk2 complexes (p27-ΔCdk) as substrates for cyclin A/Cdk2. Proteins were incubated with recombinant cyclin A/Cdk2 and γ-[^{32}P]-ATP. ^{32}P incorporation into p27 was detected by autoradiography.

(B) Y88 phosphorylation but not Y89 phosphorylation promotes T187 phosphorylation by Cdk2 in vitro. p27, p27^{Y88F}, and p27^{Y89F} were phosphorylated by recombinant Abl-kinase (+) and incubated with cyclin A/Cdk2 at 37°C for 5 min. The degree of p27 phosphorylation at T187 was detected by a phospho-T187-specific antibody. The membrane was subsequently probed with an HRP-conjugated anti-p27 antibody. The tyrosine-phosphorylation status of the p27 used in this assay was confirmed in separate western blots utilizing anti-phospho-Y88- or anti-phospho-Y89-specific antibodies.

(C) Y88 phosphorylation of p27 promotes phosphorylation of T187 by enabling a pseudo-unimolecular reaction mechanism. Total p27^{Y89F}/cyclin A/Cdk2 protein concentration dependence of the rate of phosphorylation of T187 for reactions with p27^{Y89F} and pY88-p27^{Y89F} is shown. The symbols indicate experimental data points (triangles, p27^{Y89F}; squares, pY88-p27^{Y89F}), and the solid lines illustrate curves calculated using Equation 1 (black trace for p27^{Y89F}) and Equation 2 (gray trace for pY88-p27^{Y89F}). The error bars correspond to ± one standard deviation of the mean based on triplicate measurements. See Table S1 and Supplemental Data for details of the curve-fitting procedure.

(D) T187 within a separate polypeptide (p27^{ΔN}) was phosphorylated to the same extent as T187 within p27^{Y89F} but to a significantly smaller extent than T187 within pY88-p27^{Y89F}. Experimental conditions were the same as for those illustrated in Figure 4C except that an equimolar amount of p27^{ΔN} was also included. The extent of T187 phosphorylation in pY88-p27^{Y89F} and p27^{ΔN} or p27^{Y89F} and p27^{ΔN} by Cdk2 was determined in PhosphorImager scans (see Figure S10). A mutant protein carrying alanine in position of T187 was not phosphorylated in these experiments (data not shown).

(E) Y88 phosphorylation promotes T187 phosphorylation in vivo. 293T cells transiently coexpressing either the HA-tagged WT p27 or a p27-Y88F mutant and Lyn kinase were treated with Na-orthovanadate and proteasome inhibitor for 4 hr. HA-tagged p27 was immunoprecipitated with an anti-HA antibody. Immunoprecipitates were analyzed with a phospho-T187-specific antibody. The membrane was subsequently probed with an HRP-conjugated anti-p27 antibody.

a protein phosphorylated on Y89 was not a good substrate for Cdk2-dependent phosphorylation (Figure 4B). Thus, Y88 phosphorylation primes p27 for subsequent T187 phosphorylation.

We hypothesized that Cdk2-mediated phosphorylation of pY88-p27 on T187 occurred via a pseudo-unimolecular mechanism within the *same* ternary pY88-p27/cyclin A/Cdk2 complex. To test this model, we determined the ternary complex concentration dependence of this reaction rate. At all concentrations, significant phosphorylation of pY88-p27^{Y89F} was observed (Figure 4C), while p27^{Y89F} was phosphorylated to a much smaller extent. Similar experiments were performed in the presence of a competing C-terminal fragment of p27 (residues 105–198; p27^{ΔN}), which fails to bind to the kinase complex. With the Y88-phosphorylated complex, pY88-p27^{Y89F} was

phosphorylated on T187 to a much greater extent than $p27^{\Delta N}$, while with the Y88-unphosphorylated complex, $p27^{Y89F}$ and $p27^{\Delta N}$ were phosphorylated to similar but much smaller extents (Figures 4D and S10). Mathematical analysis of the reaction rates (Figure 4C) revealed that phosphorylation of Y88 primes p27 for Cdk2-mediated phosphorylation of T187 by allowing the reaction to proceed via an unprecedented pseudo-unimolecular mechanism (shown in the Supplemental Data). Y88 phosphorylation thus promotes a transition of p27 from an inhibitor into a substrate of Cdk2.

Tyrosine Phosphorylation Primes for T187 Phosphorylation In Vivo

To investigate if phosphorylation of p27 on Y88 promoted subsequent Cdk2-mediated phosphorylation at T187 in vivo, we coexpressed constitutively active Lyn with p27 in 293T cells. Expression of Lyn strongly enhanced T187 phosphorylation of p27 in comparison to the untransformed control (Figure 4E). To eliminate the possibility that enhanced T187 phosphorylation was an indirect result of Lyn overexpression that was independent of Y88 phosphorylation, we expressed a mutant p27 protein in which Y88 was replaced by phenylalanine. Consistent with our model of the specific importance of pY88 in priming phosphorylation of T187, this mutant exhibited significantly reduced T187 phosphorylation (Figure 4E).

Imatinib Inhibits Y88 Phosphorylation of p27 by BCR-ABL

The BCR-ABL oncogene is a product of the Philadelphia translocation which causes chronic myelogenous leukemia (CML) and BCR-ABL-positive acute lymphoblastic leukemia (ALL). The constitutively active kinase induces and maintains leukemic transformation (Huettner et al., 2000). BCR-ABL is specifically inhibited by Imatinib mesylate/STI571/Gleevec (Wong and Witte, 2004). To determine if tyrosine phosphorylation of p27 directly depended on BCR-ABL kinase activity, we added STI571 to 293T cells transfected with BCR-ABL and p27. Y88 phosphorylation was barely detectable 2 hr after addition of STI571, which confirms that Y88 phosphorylation required active BCR-ABL (Figure 5A). Addition of STI571 to Lyn-transfected cells did not affect Y88 phosphorylation by Lyn (Figure 5A), which indicates that STI571 is specific for BCR-ABL and supports the hypothesis that p27 might be a specific substrate of BCR-ABL.

We next investigated Y88 phosphorylation of p27 in a BCR-ABL-transformed tumor cell line, K562. These CML cells express a p210 BCR-ABL kinase that is inhibited by STI571. Endogenous p27 of K562 cells was phosphorylated on Y88 (Figure 5B). Addition of STI571 abrogated Y88 phosphorylation (Figure 5B), suggesting that tyrosine phosphorylation of p27 depended on sustained BCR-ABL tyrosine kinase activity. In comparison to 293T cells, Y88 phosphorylation of endogenous p27 declined more slowly in STI571-treated K562 cells (compare Figures 5A, 5B, and S11). This suggests that additional tyrosine kinases that have been activated by BCR-ABL may contribute to p27 tyrosine phosphorylation. Among other tyrosine kinases, Lyn is induced by p210 BCR-ABL in hematopoietic cells

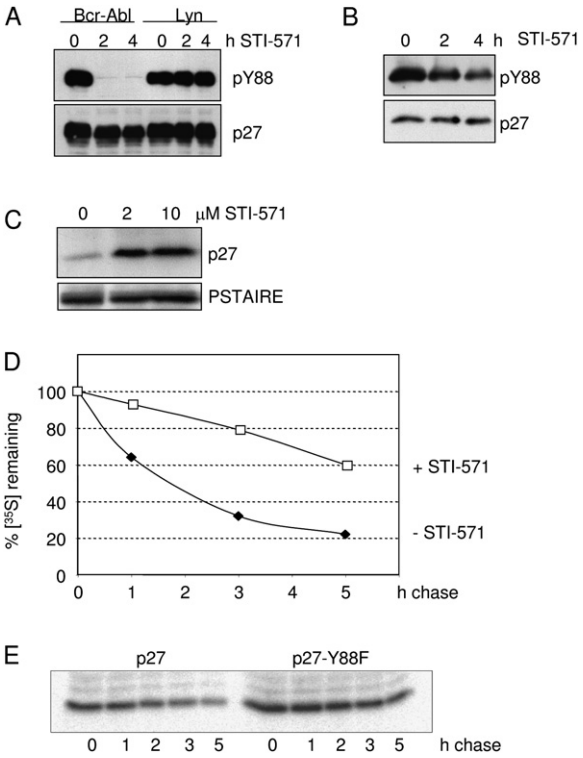

Figure 5. Inhibition of BCR-ABL reduces p27-Y88 Phosphorylation and BCR-ABL Inhibition, and Y88F Mutation Stabilizes the p27 Protein

(A) Imatinib/STI571 prevents BCR-ABL-induced p27 tyrosine phosphorylation. 293T cells were transfected with HA-tagged p27 and BCR-ABL or Lyn kinase and then treated with 10 μM STI571 for the times indicated. Equal amounts of cell lysates were analyzed by western blotting with monoclonal anti-pY88-p27 antibodies and HRP-conjugated anti-p27 antibodies as indicated.

(B) STI571 prevents tyrosine phosphorylation of endogenous p27 in K562 cells. K562 cells were treated with 10 μM STI571 for 2 and 4 hr. p27 level and Y88 phosphorylation were determined by western blotting of p27 immunoprecipitates using monoclonal anti-pY88-p27 and HRP-conjugated anti-p27 antibodies.

(C) STI571 increases p27 levels in K562 cells. Cells were treated with 2 or 10 μM STI571 for 16 hr, and equal amounts of protein were analyzed by western blotting utilizing anti-p27 and anti-PSTAIRE antibodies.

(D) STI571 increases the stability of p27 in K562 cells. K562 cells were mock-treated or treated with 10 μM STI571 for 16 hr. Cells were labeled with [^{35}S]-methionine and [^{35}S]-cysteine for 1 hr and subsequently incubated in the absence of radioactive amino acids for the times indicated. p27 was immunoprecipitated using polyclonal anti-p27 antibodies. The radioactive protein was visualized by autoradiography. The intensity of the bands was determined using a PhosphorImager and is expressed as a fraction of the time point 0. Triplicate experiments gave similar results; representative results are shown.

(E) $p27^{Y88F}$ is more stable than p27. Subconfluent cultures of $p27^{-/-}$ MEFs were retrovirally transduced with p27 or $p27^{Y88F}$ and labeled with a [^{35}S] methionine/cysteine mix for 1.5 hr. p27 was immunoprecipitated and visualized by autoradiography. One representative of three independent experiments is shown.

(Danhauser-Riedl et al., 1996). Activated Lyn and BCR-ABL may both contribute to Y88 phosphorylation of p27.

BCR-ABL Activity Destabilizes p27

Phosphorylation of p27 on T187 can initiate its Skp2-dependent ubiquitination and degradation (Bloom and Pagano, 2003). Therefore, increased T187 phosphorylation stemming from Y88 phosphorylation may explain the enhanced degradation of p27 in tumors harboring activated tyrosine kinases. Consistent with this hypothesis, the level of p27 protein was dramatically increased following STI571 treatment (Figure 5C) as described previously in BCR-ABL-transformed cells (Coutts et al., 2000; Gesbert et al., 2000; Jonuleit et al., 2000). The increase in p27 protein upon inhibition of BCR-ABL kinase by STI571 correlated with an increase in endogenous p27 stability as demonstrated in pulse-chase experiments (Figure 5D), which further supports the hypothesis that tyrosine phosphorylation primes for p27 degradation.

Mutation of Tyrosine 88 to Phenylalanine Stabilizes p27

p27 stabilization upon BCR-ABL inactivation might be a consequence of cell-cycle arrest in G_1 phase. To more directly investigate the role of Y88 phosphorylation in p27 stability, we retrovirally expressed p27 or a p27-Y88F mutant in immortalized $p27^{-/-}$ mouse embryonic fibroblasts (MEFs). p27 that can be phosphorylated on Y88 showed a half-life comparable to that described for endogenous p27 (123 min ± 20.5 min; Figure 5E). By contrast, the p27-Y88F mutant was significantly more stable (half-life of 204 min ± 21.1 min; Figure 5E). It is unlikely that stabilization of p27 results from an inability of the mutant to bind to Cdk2 complexes because we determined that $p27^{Y89F}$ and $p27^{Y88,89F}$ have similar affinities for cyclin A/Cdk2 (Figure S6 and Table 1).

$p27^{Y88F}$ Exhibited Enhanced Cdk-Inhibitory Potency In Vivo

Because pY88-p27 exhibited reduced Cdk-inhibitory activity and stability, we speculated that a mutant protein that could not be phosphorylated would be more potent in arresting BCR-ABL-transformed tumor cells. We therefore expressed p27 and $p27^{Y88F}$ in K562 cells. Conditions were adjusted to express WT and mutant p27 at similar levels (Figure 6A, right panel). Ectopic expression of p27 at a high level led to accumulation of cells in G_1 phase irrespective of the mutation of Y88F (data not shown). However, expression at an intermediate level revealed that p27 failed to arrest K562 cells in G_1 phase, whereas expression of the mutant $p27^{Y88F}$ at this level resulted in an increased number of G_1 phase cells and a reduced number of S phase cells, respectively (Figure 6A).

Y88 of p27 Is Phosphorylated in G_1 Phase

Elevated Y88 phosphorylation might be a hallmark of cancer cells and/or a regulatory mechanism that mediates progression of normal cells through the division cycle.

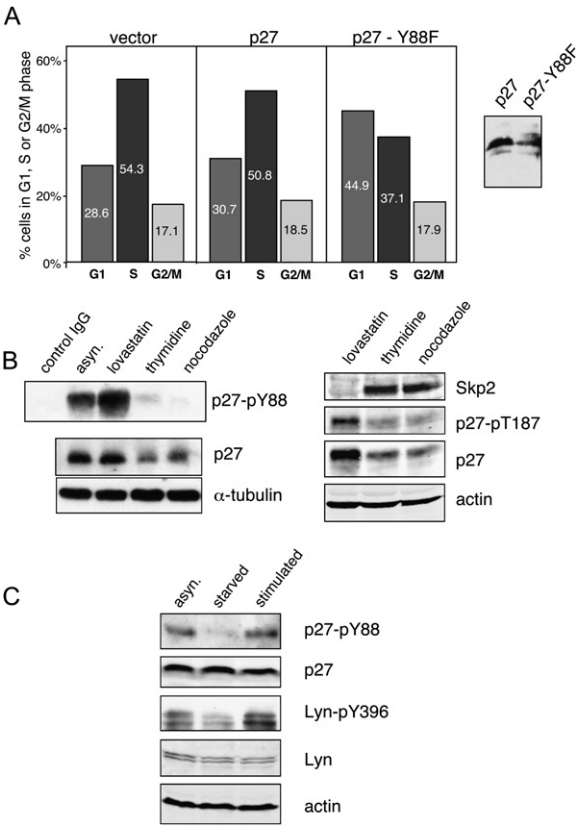

Figure 6. Tyrosine 88 Phosphorylation of p27 Is Increased in Serum-Stimulated and G1 Phase Cells

(A) $p27^{Y88F}$ is more potent than p27 in arresting K562 cells. K562 cells were electroporated with p27- or $p27^{Y88F}$-expressing vectors and a GFP-expressing vector. Expression levels of p27 are shown in the right panel. Forty-eight hours following transfection, GFP-expressing cells were isolated by cell sorting and labeled with BrdU for 3 hr. The DNA content was determined by flow cytometry after staining for DNA with propidium-iodide and for replicated DNA using anti-BrdU FITC-labeled antibodies. A representative experiment is shown.

(B) p27 is tyrosine phosphorylated in G_1 phase. Extracts of proliferating or arrested HeLa cells were analyzed for p27 Y88 phosphorylation. Tyrosine-phosphorylated p27 was immunoprecipitated using a monoclonal pY88-p27-specific antibody and was detected by western blotting using a polyclonal pY88-specific antibody. Extracts used for immunoprecipitations were analyzed by western blotting with p27- and α-tubulin-specific antibodies as indicated. Using the same protein extracts in a second blot, expression of Skp2, pT187-p27, p27, and actin were determined for cells arrested in lovastatin, thymidine, and nocodazole as shown in the right panel.

(C) Serum stimulation enhances Y88 phosphorylation. RPMI-8226 cells were starved for 24 hr in medium containing 0.2% FCS. Starved cells were stimulated with 20% FCS and 10 ng/ml IL6 for 30 min. Thirty minutes prior to stimulation all cells were treated with 1 mM Na-orthovanadate. Y88-phosphorylated p27 was precipitated using monoclonal anti-pY88-p27-specific antibodies and detected by western blotting using a p27-specific HRP-conjugated antibody. Lyn was immunoprecipitated, and active Lyn was detected with a phospho-Y396-specific antibody. p27, actin, and Lyn expression were analyzed in total cell extracts.

To investigate whether Y88 phosphorylation also regulated endogenous p27 at specific points of the cell cycle, we determined the extent of Y88 phosphorylation for p27 in HeLa cells. pY88-p27 was detected in proliferating HeLa cells (Figure 6B), and its levels were increased when cells were arrested in G_1 phase using lovastatin. Lovastatin-arrested cells did not express Skp2 and accumulated p27 phosphorylated on both Y88 and T187 (Figure 6B). By contrast, Y88 phosphorylation was reduced in cells arrested using thymidine and nocodazole in S or G_2/M phase, respectively (Figure 6B).

We also observed increased Y88 phosphorylation after stimulation of starved RPMI-8226 myeloma cells with serum and IL-6 (Figure 6C). IL-6 is a potent growth factor for plasmocytoma/myeloma cells (Kawano et al., 1988) that leads to activation of Lyn kinase (Hallek et al., 1997). Serum starvation reduced Lyn activity, and stimulation increased Lyn activity (Figure 6C). In parallel, serum starvation reduced Y88 phosphorylation, and growth-factor stimulation led to an increase in p27-Y88 phosphorylation. This is consistent with a possible contribution of specific Src-family tyrosine kinases to p27 Y88 phosphorylation.

DISCUSSION

A number of links between p27 and multiple oncogenic pathways have been established and include the Ras, Myc, and Akt/PKB pathways (Blain et al., 2003). We add here a direct link between p27 inactivation and tyrosine kinase activation. Whereas a single unmodified Cip/Kip protein is sufficient for Cdk2 inhibition (Hengst et al., 1998; Russo et al., 1996), phosphorylation of Y88 in p27 impaired its ability to inhibit the bound kinase complex, and, even in the presence of a large excess of pY88-p27, inhibitor-bound kinases retained substantial catalytic activity. This mechanism may explain previous observations of active kinase complexes coimmunoprecipitating with p27 (Blain et al., 1997; Cheng et al., 1999; Dong et al., 1998; LaBaer et al., 1997; Soos et al., 1996).

In addition, Y88 phosphorylation triggered Cdk2-mediated threonine 187 phosphorylation through a pseudo-unimolecular mechanism and initiated proteolysis of the Cdk inhibitor. This suggests that p27 Y88 phosphorylation may be one mechanism to initiate SCF-Skp2-dependent p27 degradation during the normal cell cycle. Further, this mechanism may contribute to tumor formation that involves activated tyrosine kinases. For example, p27 may be deregulated by constitutive Y88 phosphorylation in BCR-ABL-positive leukemias. While overexpressed BCR-ABL directly phosphorylates p27, BCR-ABL-activated tyrosine kinases are likely to contribute to p27 Y88 phosphorylation. One such kinase that is activated by BCR-ABL is Lyn, a tyrosine kinase that directly binds p27. In addition, we demonstrate that c-src coprecipitates with p27 (Chu et al., 2007 [this issue of Cell]). Src phosphorylates the tyrosine residues 88 and 74 of p27. In accordance with our observation reported here, phosphorylation by Src also leads to reduced stability of p27 and impaired Cdk inhibition by p27. Interestingly, Src activation correlates with low nuclear p27 in primary human breast cancers, further indicating the link between oncogenic tyrosine kinases and p27 (Chu et al., 2007 [this issue of Cell]).

The intrinsic flexibility of p27 (Lacy et al., 2004; Sivakolundu et al., 2005) enables the two-step phosphorylation cascade that triggers p27 degradation. First, intrinsic flexibility allows the Y88-phosphorylated 3_{10}-helix to rotate out of the Cdk2 active-site cleft without weakening other interactions with cyclin A/Cdk2. This Y88 phosphorylation-induced structural change transforms p27 from a Cdk inhibitor into a captive Cdk substrate. Second, extensive flexibility within the p27 C terminus enables T187 to encounter the Cdk2 active site within *the same* pY88-p27/cyclin A/Cdk2 ternary complex.

Consistent with our model, p27 levels are decreased in CML-$CD34^+$ cells as compared to normal $CD34^+$ cells (Andreu et al., 2005). Treatment with STI571 restored p27 levels. Interestingly, STI571 treatment of BCR-ABL-positive leukemia patients frequently leads to relapse due to drug-resistant clones. STI571-resistant tumor cell lines have been characterized by elevated Lyn expression (Donato et al., 2003). While STI571 inhibits Y88 phosphorylation by BCR-ABL, it fails to do so in Lyn-expressing cells (Figure 5A).

While potentially important in oncogenesis by activated tyrosine kinases, the pattern of Y88 phosphorylation during the cell cycle suggests that Y88 phosphorylation regulates p27 activity and stability in normal cells. As Y88 is conserved in all Cip/Kip family inhibitors, it will be interesting to determine whether this residue is also phosphorylated in p21 or p57. As tyrosine phosphorylation relieves Cdk inhibition by p27, this may explain observations of a number of groups that active Cdk complexes can coprecipitate with p21 and p27, hence enabling the inhibitors to act as assembly factors and, thus, activators of Cdks (Cheng et al., 1999; Sherr and Roberts, 1999).

EXPERIMENTAL PROCEDURES

Cell Culture

K562 and RPMI-8226 cells were maintained in RPMI 1640; HeLa, 293T, MCF7, and $p27^{-/-}$ MEFs were maintained in DMEM. Media were supplemented with 10% FBS, 1 mM pyruvate, 50 U/ml penicillin, and 100 μg/ml streptomycin. RPMI-8226 cells were serum starved for 24 hr in medium containing 0.2% FBS. Cell synchronization and cell-cycle analysis with BrdU and PI was performed as described (Hengst and Reed, 1996).

Phosphoamino Acid Analysis

HeLa cells expressing untagged p27 were metabolically labeled with 0.5 mCi [^{32}P]-ortho-phosphate for 4 hr. Cells were lysed, p27 immunoprecipitated with a C-terminal antibody (C-19, Santa Cruz Biotechnology), separated by SDS-PAGE, and blotted on PVDF membrane. Phosphorylated p27 was excised from the membrane and hydrolyzed in 6N HCl. Resulting free amino acids were mixed with phosphoamino acid standard (Sigma) and fractionated by 2D thin-layer chromatography (pH 1.9 and pH 3.5) as described (Boyle et al., 1991). Phosphorylated amino acids were analyzed by overlaying autoradiogram of TLC

plate with the position of amino acid standard on the same plate and were visualized by ninhydrin staining.

Antibodies

Polyclonal antibodies specific for Y88-phosphorylated p27 were generated by immunizing rabbits with the ovalbumin-coupled peptide LPEF-phosphoYYRPPR. Antisera were purified by passage on a column linked to the unphosphorylated peptide followed by purification on a column linked to the phosphorylated peptide. Antibodies against Y89-phosphorylated p27 were generated using the coupled peptide PEFYphospho-YRPPRP, and antibodies against Y88-Y89-phosphorylated p27 were generated using the peptide LPEFphospho-Yphospho-YRPPR. Monoclonal antibodies directed against Y88-phosphorylated p27 were generated using the peptide in mice. p27-pT187-specific antibodies from Zymed or from Upstate were preadsorbed with soluble recombinant p27 and were subsequently tested for crossreactivity with the unphosphorylated protein. p27 was detected and precipitated using a polyclonal antibody (C-19, Santa Cruz Biotechnology). Active Lyn was detected with a phospho-Y396-specific rabbit monoclonal antibody (Epitomics) after immunoprecipitation with a mouse monoclonal Lyn antibody (BD).

Pulse–Chase Analysis

K562 cells (1×10^7/ml) were cysteine/methionine starved for 45 min and incubated with 50 μCi/ml [^{35}S] cysteine/methionine (ProMix, Amersham) for 1 hr. Following washes, cells were incubated in isotope-free media supplemented with 0.1 mg/ml cysteine and 0.1 mg/ml methionine then analyzed as described (Hengst and Reed, 1996). p27$^{-/-}$ MEFs stably expressing Lyn (Y508F) were retrovirally transduced with p27 or a p27-Y88F mutant. Cells were starved for 45 min, labeled with a [^{35}S] cysteine/methionine for 1.5 hr, and analyzed as described above.

Protein Expression and Analysis; Kinase and Phosphatase Reactions

p27 cDNAs were expressed in *E. coli*. Human Cdk2 and full-length cyclin A were purified from baculovirus-infected Sf9 cells. In kinase reactions, p27 was added to cyclin A/Cdk2. To determine IC50 at elevated p27 level, 1.5 ng/μl and 0.3 ng/μl kinase were used. A baculovirus encoding cyclin D1 and Cdk4 as a single polypeptide linked by a polyalanine sequence was expressed in Sf9 cells. The SH3 and kinase domains of murine Abl were amplified by PCR, subcloned into pET28a-vector, expressed, and purified from *E. coli*. Human Lyn was purchased from Sigma and Upstate.

Tyrosine phosphorylation by Abl or Lyn kinases was performed for up to several hours at 37°C in a buffer containing 20 mM HEPES (pH 7.5), 250 mM NaCl, 5 mM $MgCl_2$, 1 mM $MnCl_2$, 0.05% NP40, 7.15 mM β-mercaptoethanol, 125 μM Na-orthovanadate, protease inhibitors, and 1 mM ATP. Radioactive kinase reactions were performed at 30°C for 45–90 min with 10 μCi γ-[^{32}P]-ATP and 25 μM cold ATP. For subsequent reactions, Y-phosphorylated p27 was repurified by including a step of heat denaturation (100°C; 10 min.) to inactivate the tyrosine kinase. Activity of recombinant cyclin/Cdk complexes was determined as described (Hengst et al., 1998). Gel filtration analysis was performed on a Sephadex 200 HR column in 150 mM NaCl, 50 mM Tris (pH 7.5), 1 mM PMSF, and 1 mM DTT. Fractions (0.5 ml) were collected at a flow rate of 0.6 ml/min at 4°C by isocratic elution over 1.5 column volumes. Fractions were analyzed using SDS-PAGE with Coomassie or western blot detection.

Protein Expression and Purification for SPR, NMR, and In Vitro Kinase Assays

cDNA for residues 22–104 (p27-KID), 105–198 (p27$^{\Delta N}$), and 1–198 (full-length) of human p27 were subcloned into pET28a (Novagen). Similar constructs were prepared with Y89 mutated to F. These proteins, human Cdk2, T160-phosphorylated Cdk2, and truncated human cyclin A (residues 173–432 of human cyclin A) were expressed in *E. coli* and purified as described (Lacy et al., 2004). Y88-phosphorylated p27-KID^{Y89F} and p27^{Y89F} were prepared by incubating Abl kinase domain and the p27 samples at 30°C for 2 hr followed by Fe^{3+}-affinity chromatography. Isotope-labeled samples of p27-KID and p27 were prepared as described (Neidhardt et al., 1974) using ^{15}N-ammonium chloride, ^{13}C-glucose, and ^2H_2O. To produce p27-KID labeled at specific amino acids with ^{15}N, an auxotrophic *E. coli* strain DL39(DE3) was cultured in MOPS-based minimal media supplemented with amino acids (Waugh, 1996).

SPR Experiments

Kinetic studies were performed using a BIACORE 3000 (Biacore, Inc.) SPR instrument. p27 polypeptides were immobilized as previously reported (Lacy et al., 2004) and as given under Supplemental Data. The kinetics of association and dissociation to immobilized p27 species were monitored using 20–2000 nM Cdk2, 3.9–250 nM cyclin A, and 0.4–40 nM cyclin A/Cdk2 complex. Data from triplicate injections for each analyte were analyzed by simultaneously fitting association phases and dissociation phases at all concentrations using the program CLAMP (Myszka and Morton, 1998) with a 1:1 binding model. The association rate constants and dissociation rate constants (k_a and k_d, respectively) for Cdk2 binding to p27 constructs were used to calculate the corresponding equilibrium dissociation constants (K_D) using $K_D = k_d / k_a$. The binding of cyclin A and cyclin A/Cdk2 to the p27 species exhibited biphasic kinetics; therefore, binding isotherms were generated from the response at equilibrium for each injection, and K_D values were determined using the program Scrubber (Version 1.1g, BioLogic Software).

NMR Spectroscopy

p27 polypeptides and their complexes with cyclin A/Cdk2 were analyzed using NMR spectroscopy at 800 MHz using methods described previously (Wang et al., 2005) and as reported under Supplemental Data.

In Vitro Cdk2 Kinase Activity Assays and Kinetic Studies of T187 Phosphorylation

The inhibitory profiles of p27 and pY88-p27 species were determined by measuring in vitro Cdk2 kinase activity toward histone H1 in the presence of different concentrations of p27-KID^{Y89F}, p27^{Y89F}, and their Y88-phosphorylated analogs. The experimental details are given under Supplemental Data. Kinetic analysis of the T187-phosphorylation reaction mechanisms was performed with five different concentrations (0.25, 0.5, 1.0, 2.0, and 4.0 μM) of p27^{Y89F}/cyclin A/Cdk2 and pY88-p27^{Y89F}/cyclin A/Cdk2. These reagents were equilibrated with γ-[^{32}P]-ATP for four time intervals (20, 40, 60, and 120 min) and were followed by analysis using SDS-PAGE. In addition, similar reactions were performed for 40 min in the presence of equimolar concentrations (with respect to ternary complex constituents) of p27$^{\Delta N}$.

Supplemental Data

Supplemental Data include equations, Supplemental Experimental Procedures, 13 figures, and two tables and can be found with this article online at http://www.cell.com/cgi/content/full/128/2/269/DC1/.

ACKNOWLEDGMENTS

We thank Steven I. Reed for a baculovirus expressing a single-chain cyclin D1/Cdk4. We also thank Nisar P. Malek and James M. Roberts for a p27$^{-/-}$ MEF cell line, Axel Ullrich for Grb2 and Abl cDNA expression vectors, Markus Warmuth for a Lyn cDNA, and Ottmar J. Janssen for SH3 domain expression plasmids. We are grateful to Alicia Baskaya and Hans Brandstetter for support in antibody production and to Silva Andric, Luis Moroder, and Bob Cassell for peptide synthesis. We especially thank Wolfgang Klinkert for cell sorting and Garnet Bendig for stimulating discussions. Finally, Limin Xiao is thanked for preparation of p27 proteins for NMR studies, Jack Sublett for assistance with

p27-phosphorylation studies, and Clive Slaughter and Ashutosh Mishra for performing the mass spectrometry analysis. This work was supported by grants to L.H. from the Regierung von Oberbayern, Roche Diagnostics, and the Max Planck Society as well as FWF grant P18873. R.W.K. acknowledges support from the American Lebanese Syrian Associated Charities (ALSAC) and NIH through P30 CA21765 (to St. Jude Children's Research Hospital), R01 CA82491, and RR014675 (for the Biacore 3000 instrument). A patent application related to the wave presented in the paper was submitted by the authors.

Received: May 11, 2006
Revised: September 13, 2006
Accepted: November 20, 2006
Published: January 25, 2007

REFERENCES

Andreu, E.J., Lledo, E., Poch, E., Ivorra, C., Albero, M.P., Martinez-Climent, J.A., Montiel-Duarte, C., Rifon, J., Perez-Calvo, J., Arbona, C., et al. (2005). BCR-ABL induces the expression of Skp2 through the PI3K pathway to promote p27Kip1 degradation and proliferation of chronic myelogenous leukemia cells. Cancer Res. *65*, 3264–3272.

Blain, S.W., Montalvo, E., and Massague, J. (1997). Differential interaction of the cyclin-dependent kinase (Cdk) inhibitor p27Kip1 with cyclin A-Cdk2 and cyclin D2-Cdk4. J. Biol. Chem. *272*, 25863–25872.

Blain, S.W., Scher, H.I., Cordon-Cardo, C., and Koff, A. (2003). p27 as a target for cancer therapeutics. Cancer Cell *3*, 111–115.

Bloom, J., and Pagano, M. (2003). Deregulated degradation of the cdk inhibitor p27 and malignant transformation. Semin. Cancer Biol. *13*, 41–47.

Boyle, W.J., van der Geer, P., and Hunter, T. (1991). Phosphopeptide mapping and phosphoamino acid analysis by two-dimensional separation on thin-layer cellulose plates. Methods Enzymol. *201*, 110–149.

Cheng, M., Olivier, P., Diehl, J.A., Fero, M., Roussel, M.F., Roberts, J.M., and Sherr, C.J. (1999). The p21(Cip1) and p27(Kip1) CDK 'inhibitors' are essential activators of cyclin D-dependent kinases in murine fibroblasts. EMBO J. *18*, 1571–1583.

Chu, I., Sun, J., Anaout, A., Kahn, H., Hanna, W., Narod, S., Sun, P., Tan, C.-K., Hengst, L., and Slingerland, J. (2007). p27 phosphorylation by Src regulates inhibition of Cyclin E-Cdk2. Cell *128*, this issue, 281–294.

Ciarallo, S., Subramaniam, V., Hung, W., Lee, J.H., Kotchetkov, R., Sandhu, C., Milic, A., and Slingerland, J.M. (2002). Altered p27(Kip1) phosphorylation, localization, and function in human epithelial cells resistant to transforming growth factor beta-mediated G(1) arrest. Mol. Cell. Biol. *22*, 2993–3002.

Coutts, M., Zou, X., and Calame, K. (2000). v-Abl utilizes multiple mechanisms to drive G1/S progression in fibroblasts. Oncogene *19*, 801–809.

Danhauser-Riedl, S., Warmuth, M., Druker, B.J., Emmerich, B., and Hallek, M. (1996). Activation of Src kinases p53/56lyn and p59hck by p210bcr/abl in myeloid cells. Cancer Res. *56*, 3589–3596.

Donato, N.J., Wu, J.Y., Stapley, J., Gallick, G., Lin, H., Arlinghaus, R., and Talpaz, M. (2003). BCR-ABL independence and LYN kinase overexpression in chronic myelogenous leukemia cells selected for resistance to STI571. Blood *101*, 690–698.

Dong, F., Agrawal, D., Bagui, T., and Pledger, W.J. (1998). Cyclin D3-associated kinase activity is regulated by p27kip1 in BALB/c 3T3 cells. Mol. Biol. Cell *9*, 2081–2092.

Gesbert, F., Sellers, W.R., Signoretti, S., Loda, M., and Griffin, J.D. (2000). BCR/ABL regulates expression of the cyclin-dependent kinase inhibitor p27Kip1 through the phosphatidylinositol 3-Kinase/AKT pathway. J. Biol. Chem. *275*, 39223–39230.

Hall, M., Bates, S., and Peters, G. (1995). Evidence for different modes of action of cyclin-dependent kinase inhibitors: p15 and p16 bind to kinases, p21 and p27 bind to cyclins. Oncogene *11*, 1581–1588.

Hallek, M., Neumann, C., Schaffer, M., Danhauser-Riedl, S., von Bubnoff, N., de Vos, G., Druker, B.J., Yasukawa, K., Griffin, J.D., and Emmerich, B. (1997). Signal transduction of interleukin-6 involves tyrosine phosphorylation of multiple cytosolic proteins and activation of Src-family kinases Fyn, Hck, and Lyn in multiple myeloma cell lines. Exp. Hematol. *25*, 1367–1377.

Hengst, L., and Reed, S.I. (1996). Translational control of p27Kip1 accumulation during the cell cycle. Science *271*, 1861–1864.

Hengst, L., and Reed, S.I. (1998). Inhibitors of the Cip/Kip family. Curr. Top. Microbiol. Immunol. *227*, 25–41.

Hengst, L., Göpfert, U., Lashuel, H.A., and Reed, S.I. (1998). Complete inhibition of Cdk/cyclin by one molecule of p21(Cip1). Genes Dev. *12*, 3882–3888.

Huettner, C.S., Zhang, P., Van Etten, R.A., and Tenen, D.G. (2000). Reversibility of acute B-cell leukaemia induced by BCR-ABL1. Nat. Genet. *24*, 57–60.

Jonuleit, T., van der Kuip, H., Miething, C., Michels, H., Hallek, M., Duyster, J., and Aulitzky, W.E. (2000). Bcr-Abl kinase down-regulates cyclin-dependent kinase inhibitor p27 in human and murine cell lines. Blood *96*, 1933–1939.

Kamura, T., Hara, T., Matsumoto, M., Ishida, N., Okumura, F., Hatakeyama, S., Yoshida, M., Nakayama, K., and Nakayama, K.I. (2004). Cytoplasmic ubiquitin ligase KPC regulates proteolysis of p27(Kip1) at G1 phase. Nat. Cell Biol. *6*, 1229–1235.

Kardinal, C., Dangers, M., Kardinal, A., Koch, A., Brandt, D.T., Tamura, T., and Welte, K. (2006). Tyrosine phosphorylation modulates binding preference to cyclin-dependent kinases and subcellular localization of p27Kip1 in the acute promyelocytic leukemia cell line NB4. Blood *107*, 1133–1140.

Kawano, M., Hirano, T., Matsuda, T., Taga, T., Horii, Y., Iwato, K., Asaoku, H., Tang, B., Tanabe, O., Tanaka, H., et al. (1988). Autocrine generation and requirement of BSF-2/IL-6 for human multiple myelomas. Nature *332*, 83–85.

Kotoshiba, S., Kamura, T., Hara, T., Ishida, N., and Nakayama, K.I. (2005). Molecular dissection of the interaction between p27 and KPC, the ubiquitin ligase that regulates proteolysis of p27 in G1 phase. J Biol Chem. *280*, 17694–17700.

LaBaer, J., Garrett, M.D., Stevenson, L.F., Slingerland, J.M., Sandhu, C., Chou, H.S., Fattaey, A., and Harlow, E. (1997). New functional activities for the p21 family of CDK inhibitors. Genes Dev. *11*, 847–862.

Lacy, E.R., Filippov, I., Lewis, W.S., Otieno, S., Xiao, L., Weiss, S., Hengst, L., and Kriwacki, R.W. (2004). p27 binds cyclin-CDK complexes through a sequential mechanism involving binding-induced protein folding. Nat. Struct. Mol. Biol. *11*, 358–364.

Moeller, S.J., Head, E.D., and Sheaff, R.J. (2003). p27Kip1 inhibition of GRB2-SOS formation can regulate Ras activation. Mol. Cell. Biol. *23*, 3735–3752.

Myszka, D.G., and Morton, T.A. (1998). CLAMP: a biosensor kinetic data analysis program. Trends Biochem. Sci. *23*, 149–150.

Neidhardt, F.C., Bloch, P.L., and Smith, D.F. (1974). Culture medium for enterobacteria. J Bacteriol. *119*, 736–747.

Pagano, M., Tam, S.W., Theodoras, A.M., Beer-Romero, P., Del Sal, G., Chau, V., Yew, P.R., Draetta, G.F., and Rolfe, M. (1995). Role of the ubiquitin-proteasome pathway in regulating abundance of the cyclin-dependent kinase inhibitor p27. Science *269*, 682–685.

Pavletich, N.P. (1999). Mechanisms of cyclin-dependent kinase regulation: structures of Cdks, their cyclin activators, and Cip and INK4 inhibitors. J. Mol. Biol. *287*, 821–828.

Radeva, G., Petrocelli, T., Behrend, E., Leung-Hagesteijn, C., Filmus, J., Slingerland, J., and Dedhar, S. (1997). Overexpression of the

integrin-linked kinase promotes anchorage- independent cell cycle progression. J. Biol. Chem. *272*, 13937–13944.

Russo, A.A., Jeffrey, P.D., Patten, A.K., Massague, J., and Pavletich, N.P. (1996). Crystal structure of the p27Kip1 cyclin-dependent-kinase inhibitor bound to the cyclin A-Cdk2 complex. Nature *382*, 325–331.

Sabile, A., Meyer, A.M., Wirbelauer, C., Hess, D., Kogel, U., Scheffner, M., and Krek, W. (2006). Regulation of p27 degradation and S-phase progression by Ro52 RING finger protein. Mol. Cell. Biol. *26*, 5994–6004.

Schulman, B.A., Lindstrom, D.L., and Harlow, E. (1998). Substrate recruitment to cyclin-dependent kinase 2 by a multipurpose docking site on cyclin A. Proc. Natl. Acad. Sci. USA *95*, 10453–10458.

Sherr, C.J., and Roberts, J.M. (1999). CDK inhibitors: positive and negative regulators of G1-phase progression. Genes Dev. *13*, 1501–1512.

Sivakolundu, S.G., Bashford, D., and Kriwacki, R.W. (2005). Disordered $p27^{Kip1}$ exhibits intrinsic structure resembling the Cdk2/cyclin A-bound conformation. J Mol Biol. *353*, 1118–1128. Published online September 20, 2005. 10.1016/j.jmb.2005.08.074.

Soos, T.J., Kiyokawa, H., Yan, J.S., Rubin, M.S., Giordano, A., DeBlasio, A., Bottega, S., Wong, B., Mendelsohn, J., and Koff, A. (1996). Formation of p27-CDK complexes during the human mitotic cell cycle. Cell Growth Differ. *7*, 135–146.

Sugiyama, Y., Tomoda, K., Tanaka, T., Arata, Y., Yoneda-Kato, N., and Kato, J. (2001). Direct binding of the signal-transducing adaptor Grb2 facilitates down-regulation of the cyclin-dependent kinase inhibitor p27Kip1. J. Biol. Chem. *276*, 12084–12090.

Wang, Y., Filippoy, I., Richter, C., Luo, R., and Kriwacki, R.W. (2005). Solution NMR studies of an intrinsically unstructured protein within a dilute, 75 kDa eukaryotic protein assembly; probing the practical limits for efficiently assigning polypeptide backbone resonances. Chembiochem. *6*, 2242–2246.

Waugh, D.S. (1996). Genetic tools for selective labeling of proteins with alpha-15N-amino acids. J. Biomol. NMR *8*, 184–192.

Wong, S., and Witte, O.N. (2004). The BCR-ABL story: bench to bedside and back. Annu. Rev. Immunol. *22*, 247–306.